JACS
JOURNAL OF THE AMERICAN CHEMICAL SOCIETY
Article
pubs.acs.org/JACS

Compound I Is the Reactive Intermediate in the First Monooxygenation Step during Conversion of Cholesterol to Pregnenolone by Cytochrome P450scc: EPR/ENDOR/Cryoreduction/Annealing Studies

Roman Davydov,[†] Andrey A. Gilep,[‡] Natallia V. Strushkevich,[§] Sergey A. Usanov,*[,‡] and Brian M. Hoffman*[,†]

[†]Department of Chemistry, Northwestern University, 2145 Sheridan Road, Evanston, Illinois 60208, United States
[‡]Institute of Bioorganic Chemistry, National Academy of Sciences of Belarus, 220141 Minsk, Kuprevicha 5, Belarus
[§]Structural Genomics Consortium, University of Toronto, 101 College Street, Toronto, Ontario M5G 1L7, Canada

Supporting Information

ABSTRACT: Cytochrome P450scc (CYP11A1) catalyzes conversion of cholesterol (CH) to pregnenolone, the precursor to all steroid hormones. This process proceeds via three sequential monooxygenation reactions: two stereospecific hydroxylations with formation first of 22*R*-hydroxycholesterol (22-HC) and then 20*α*,22*R*-dihydroxycholesterol (20,22-DHC), followed by C20−C22 bond cleavage. Herein we have employed EPR and ENDOR spectroscopy to characterize the intermediates in the first hydroxylation step by 77 K radiolytic one-electron cryoreduction and subsequent annealing of the ternary oxy-cytochrome P450scc-cholesterol complex. This approach is fully validated by the demonstration that the cryoreduced ternary complex of oxy-P450scc-CH is catalytically competent and hydroxylates cholesterol to form 22-HC with no detectable formation of 20-HC, just as occurs under physiological conditions. Cryoreduction of the ternary complex trapped at 77 K produces predominantly the hydroperoxy-ferriheme P450scc intermediate, along with a minor fraction of peroxo-ferriheme intermediate that converts into a new hydroperoxo-ferriheme species at 145 K. This behavior reveals that the distal pocket of the parent oxy-P450scc-cholesterol complex exhibits an efficient proton delivery network, with an ordered water molecule H-bonded to the distal oxygen of the dioxygen ligand. During annealing of the hydroperoxy-ferric P450scc intermediates at 185 K, they convert to the primary product complex in which CH has been converted to 22-HC. In this process, the hydroperoxy-ferric intermediate decays with a large solvent kinetic isotope effect, as expected when proton delivery to the terminal O leads to formation of Compound I (Cpd I). ^{1}H ENDOR measurements of the primary product formed in deuterated solvent show that the heme Fe(III) is coordinated to the 22*R*-O^{1}H of 22-HC, where the ^{1}H is derived from substrate and exchanges to D after annealing at higher temperatures. These observations establish that Cpd I is the agent that hydroxylates CH, rather than the hydroperoxy-ferric heme.

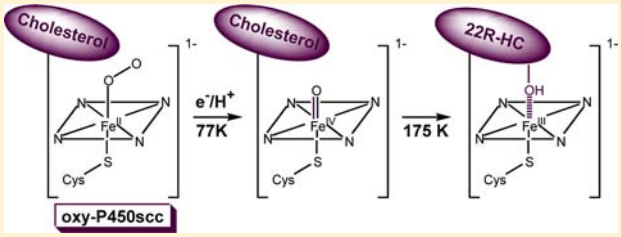

INTRODUCTION

The main precursor of all steroid hormones in vertebrates is pregnenolone, which is formed from cholesterol via three monooxygenation reactions successively catalyzed by cytochrome P450scc (CYP11A1).[1−3] During the first step, cholesterol (CH) is hydroxylated to 22*R*-hydroxycholesterol (22-HC), which in the second step is converted into 20*α*,22*R*-dihydroxycholesterol (20,22-DHC). Cleavage of the C20−C22 bond in the third step produces pregnenolone. To our knowledge the active oxygen species has not been experimentally established for any one of these three steps of hydroxylation. By analogy with other cytochrome P450 reactions, one might expect that in the first step or two Compound I (Cpd I) is the hydroxylating intermediate, while the last step might proceed with the peroxo-ferric intermediate as the active species.[4−9] On the other hand, experiments on the cryoreduction of oxy-CYP19 reported recently by Sligar and coworkers suggested that the peroxo intermediate, rather than Cpd I, is catalytically competent in the hydroxylation of androstenedione to form 19-OH-androstenedione.[10]

Despite many efforts, direct observation and detailed characterization of the catalytically active intermediates in the monooxygenase reactions of cytochromes P450 remain elusive. There have been reports of short-lived species with optical spectra characteristic of a Cpd I that are generated during reaction of cytochromes P450 with mCPBA, and that are proposed as hydroxylating species in the monooxygenase cycle.[11,12] Only recently, Rittle and Green have managed for the first time to freeze-trap Cpd I, formed in the absence of a

Received: July 10, 2012
Published: October 5, 2012

   dx.doi.org/10.1021/ja3067226 | J. Am. Chem. Soc. 2012, 134, 17149−17156

bound substrate during reaction of CYP119 with mCPBA, and to study its electron paramagnetic resonance (EPR) and Mossbauer spectra and reactivity.[13] The crystallographic structures for binary complexes of ferric cytochromes P450 with substrate allow insights, and the structures of P450scc with bound CH and 22-HC reveal how the active site of this hemeprotein is organized to bind both this initial substrate and its hydroxylation product (Figure 1).[14,15] However, these

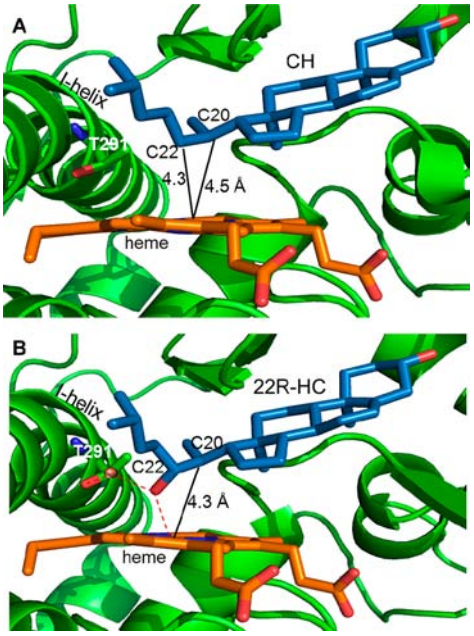

Figure 1. Active site of cytochrome P450scc (CYP11A1) in complex with (A) cholesterol (CH, PDB ID 3N9Y) and (B) 22*R*-hydroxycholesterol (22-HC, PDB ID 3N9Z). Water molecules within the active site are represented as red spheres; dashed lines indicate hydrogen bonds; solid lines indicate distance from heme iron to carbon atoms of CH substrate or 22-HC intermediate (position of subsequent hydroxylation).

equilibrium structures do not themselves imply a mechanism of the initial monooxygenation reaction. Crystallographic studies with cryoreduced oxy-P450-substrate complexes represent an extremely informative and promising approach, although experimentally quite challenging, but have not been successfully applied to P450scc.[16−18] We have previously demonstrated that application of a cryoreduction/annealing protocol in combination with EPR/electron nuclear double resonance (ENDOR) spectroscopy allows an identification of the active species in the catalytic cycle of a heme-monooxygenase.[8] Herein, application of this approach demonstrates that Cpd I is the reactive heme state in the hydroxylation of CH by P450scc to form 22-HC.

MATERIAL AND METHODS

Chemicals. Cholesterol (CH), 20α-hydroxycholesterol (20-HC), 22*R*-hydroxycholesterol (22-HC), sodium dithionite, hydroxypropyl-β-cyclodextrin, sodium cholate, glycerol, and glycerol-$d_3$were from Sigma-Aldrich. D_2O was obtained from Cambridge Isotope Laboratories Inc. O_2 was purchased from Cryogenic Gas Co.

Sample Preparation. Mature bovine recombinant P450scc was expressed, purified, and concentrated as described.[19,20] All experiments on cryoreduction were conducted using 0.25 mM oxy-P450scc in 33% glycerol (v/v)−buffer mixture containing 0.6 M NaCl, 0.04 mM KPi (pH 7.5), 0.2% sodium cholate, and 1 mM CH. When needed, the protein was exchanged into buffers made using D_2O and glycerol-d_3. In D_2O samples, the pH was adjusted to pH 7.1.[21] Final concentration of CH was achieved by adding the required volume of stock solution of 10 mM CH in 45% aqueous solution of hydroxypropyl-β-cyclodextrin to the protein solution.

The preparation of oxy-P450scc-CH complex was conducted using a modification of the procedure described by Tuckey.[22] The ferrous P450scc samples were made first by incubating the ferric protein in aqueous buffer containing 1.6 mM CH in an anaerobic glovebox overnight at 3 °C to remove oxygen from the protein solution. An aliquot of a standardized solution of sodium dithionite was added to reduce the ferric P450scc, using 10% excess of dithionite. An extinction coefficient of 8000 M^{-1} cm^{-1} at 315 nm was used to determine the concentration of dithionite. The reduced protein solution was then mixed with oxygen-free glycerol. Complete reduction of protein was confirmed spectrophotometrically. The sample of Fe(II)P450scc containing 1 mM CH was transferred into EPR tubes. Oxy-P450scc complexes were made by bubbling the Fe(II)P450scc sample at −11 °C with 20 mL of cold oxygen gas for 40−60 s (under these conditions the half-time of autoxidation of the oxy complex is ∼10 min[22]). The samples were then stored in quartz EPR tubes at 77 K until cryoreduction.

Gamma irradiation of the frozen hemoprotein solutions at 77 K typically was performed for ∼20 h (dose rate of 0.1 Mrad/h, total dose 2 Mrad) using a Gammacell 220 ^{60}Co. Annealing at temperatures over the range 77−270 K was performed by placing the EPR sample in the appropriate bath (e.g., *n*-pentane or methanol cooled with liquid nitrogen) and then refreezing in liquid nitrogen.

Spectroscopic Techniques. EPR/ENDOR measurements of samples were conducted as previously described.[23,24] UV−vis spectra of the samples in 4 mm o.d. quartz tubes were measured at 77 K through immersion in a liquid N_2 finger dewar with a USB 2000 spectrophotometer (Ocean Optics, Inc.).[23]

RESULTS

Effect of Substrates on EPR/ENDOR of Ferri-cytochrome P450scc Heme Site. We have studied the effect of substrates and products on the EPR/ENDOR spectra of ferric P450scc to provide a reference for assigning specific states that arise during cryoreduction/annealing of the tertiary oxy-P450scc-substrate complex.

The low-temperature EPR spectrum of ferric P450scc in the presence of CH exhibits a high-spin (S = 5/2) EPR signal, $\mathbf{g}$ = [8.09, 3.59, 1.69], plus a weak low-spin (S = 1/2) signal, $\mathbf{g}$ = [2.43, 2.25, 1.917] (Table 1, Figure S1). The high-spin signal is

Table 1. g-Tensor Components for Fe(III) P450scc Complexes

substrate	species	g_1	g_2	g_3
CH	low-spin	2.43	2.25	1.917
	high-spin	8.09	3.59	1.69
22-HC	major	*2.467*	*2.255*	*1.908*
	minor	2.443	2.255	1.917
20-HC		2.41	2.246	1.924

assigned to the conformational sub-state with penta-coordinated heme iron(III), as seen in the crystal structure (Figure 1); the low-spin signal is characteristic of a minority hexa-coordinate aquo-ferric form. The signals are very similar to those reported for P450scc isolated from bovine adrenocortical mitochondria.[25,26] The presence of a coordinated water in the low-spin conformer of the complex is confirmed by ^{1}H ENDOR spectra, which exhibit a signal from exchangeable proton(s) of the bound water, with maximum hyperfine

dx.doi.org/10.1021/ja3067226 | J. Am. Chem. Soc. 2012, 134, 17149−17156

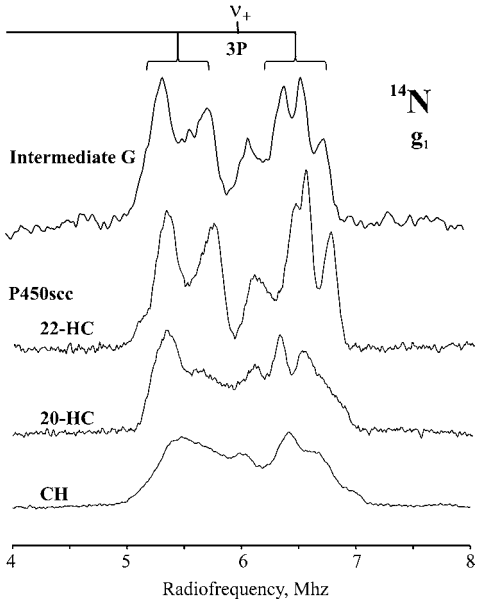

Figure 2. ^{14}N 35 GHz CW ENDOR spectrum (ν_+ − branch) of the complexes of ferric P450scc with CH, 22-CH, and 20-CH and the intermediate **G**, taken at respective g_1. Conditions: 2 K, 2 G, rf sweep rate = 0.2 MHz/s, bandwidth broadening = 20 kHz.

coupling $A \cong 8.5$ MHz lying along g_1 (Figure S3), as seen in other aquo-ferric heme complexes.[24] The appearance of a low-spin state at low temperature was observed for other substrate-bound ferri-cytochromes P450cam.[27]

The binary complex of 22-HC with Fe(III) P450scc shows low-spin EPR signals from two conformational sub-states, with **g**(1) = [2.467, 2.255, 1.908] (major, ∼75% of total protein) and **g**(2) = [2.443, 2.255, 1.917] (minor) (Table 1, Figure S2), in agreement with a previous report.[25] The major signal may be assigned to a state with 22-HC bound to the ferric heme through the hydroxyl group; the minor signal may be a second conformer of bound 22-HC, but also could be the aquo-ferric heme form. Interestingly, the relative intensities of the signals are found to change in deuterated solvent (not shown). The crystal structure for the complex of ferric P450scc with 22-HC (Figure 1)[14,15] shows the 22*R*-hydroxyl located in close proximity to the heme iron, with a reported distance of ∼2.6 A, suggesting formation of a coordination bond as indicated by EPR for the majority low-spin form.

The 2D field-frequency pattern of ^{1}H ENDOR signals collected across the EPR envelope of the low-spin EPR signal of the complex with 22-HC is considerably different and better resolved (Figure S4) as compared to that for complex ferric P450scc-CH (Figure S3). The spectrum collected at the field that corresponds to g_1 for the majority conformation shows two resolved ^{1}H ENDOR signals, with A_{max} = 4.8 and 8.3 MHz. The latter disappears in deuterated solvent and is assigned to the iron-coordinated 22*R*-hydroxyl proton; the non-exchangeable signal with A = 4.8 MHz is assigned to the ^{1}H atom of substrate closest to the Fe(III), at either the C-22 or C20 position.[28]

In agreement with a previous report,[25] the other possible product of the hydroxylation of CH, 20-HC, forms only a single low-spin complex with P450scc, with **g** = [2.416, 2.248, 1.924] (Table 1, Figure S2). The crystal structure for this complex reveals that the 20-hydroxyl is positioned away from the heme iron (distance 3.7 A) and is hydrogen-bonded to a water molecule coordinated to the heme iron.[14] Correspondingly, the

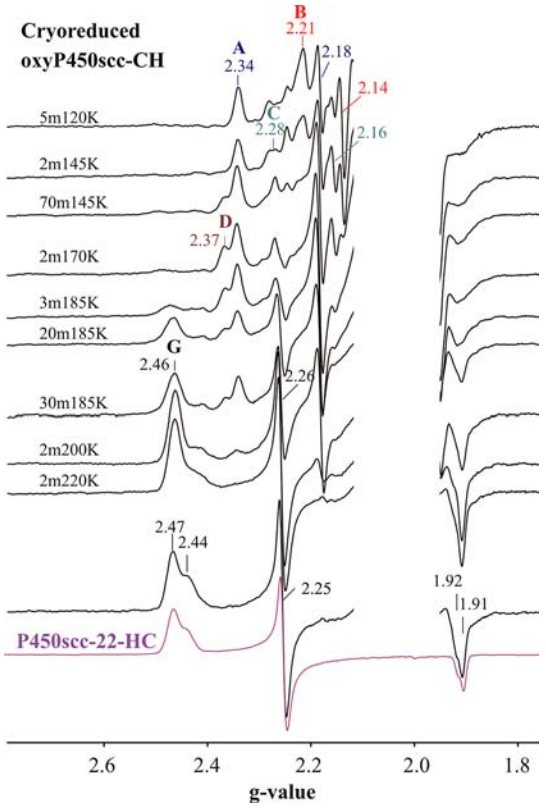

Figure 3. EPR spectra of cryoreduced oxy P450scc-CH ternary complex and after annealing steps at indicated temperatures. (For clarity the EPR signal from residual low-spin ferric P450scc available in the spectra was subtracted, and radiolytically induced radical signal was omitted.) For comparison, in the bottom of the figure, the EPR spectrum of the complex of ferri-P450scc with 22-CH is presented. Conditions: T = 25 K, 9.360 GHz, 13 W, 10 G.

^{1}H ENDOR pattern for this water ligand is similar, although not identical, to that for Fe(III)-coordinated water of ferric P450scc in the presence of CH (Figure S5).

Figure 2 shows the ^{14}N ENDOR spectra of the pyrrole nitrogens of the majority complex of ferric P450scc with CH, 22-HC, and 20-HC and the intermediate **G** (see below). The signals represent the quadrupole-split (3*P*), $\nu_+ = A/2 + \nu_N$ branch of the ^{14}N response. We specifically note that the pyrrole ^{14}N ENDOR spectra are distinctly sharpened when H_2O bound to the ferriheme of the CH and 20-HC complexes is replaced by the 22*R*-hydroxyl of 22-HC, indicating a more sharply defined structure in this latter complex (Figure 2). The signals show overlapping responses from what appear to be four similar but distinguishable ^{14}N ligands, indicating a complete symmetry lowering of the heme iron coordination environment in this complex. We consider as being less likely the alternative interpretation, that the multiplicity of signals come from relatively symmetric heme in multiple conformational sub-states, because the CH and 20-HC complexes show only a single sub-state in their low-spin EPR spectra (Figure S2), and the 22-HC complex, which shows two sub-states in the EPR spectrum, is interrogated at a field where only the dominant sub-state contributes. The average hyperfine couplings and quadrupole splittings in all cases are $A(g_1) \approx 6$ MHz and $3P(g_1) \approx 2$ MHz.

Cryoreduced Ternary Complex Oxy-P450scc-Cholesterol. Figure 3 presents EPR spectra of the oxy-P450scc-CH

dx.doi.org/10.1021/ja3067226 | J. Am. Chem. Soc. 2012, 134, 17149−17156

ternary complex after exposure to γ-irradiation at 77 K and annealing the cryogenerated intermediate at indicated temperatures between 145 and 220 K. The spectrum of the cryoreduced complex trapped at 77 K displays three distinct EPR signals. The main signal **A**, which accounts for approximately 70% of the reduced oxy-ferro heme centers (Figure S6), has **g** = [2.34, 2.18, 1.95] (Table 2), characteristic

Table 2. g-Values for 77 K Cryoreduced Oxy-P450scc-CH Complex and the Intermediates Arising during Its Annealing

species	T (K)	g_1	g_2	g_3
A (major)	77	2.34	2.182	1.949
B (minor)	77	2.214	2.14	nd
C (minor)	77	2.28	2.156	nd
D	170	2.366	2.182	1.95
G	185	2.463	2.257	1.908
E (major)	220	2.467	2.254	1.907
E (minor)	220	2.443	2.254	1.918

of hydroperoxo-ferriheme intermediate.[8,28−30] The intermediate exhibits a resolved proton ENDOR signal with $A_{max} \approx 10$ MHz that disappears in deuterated solvent and is assignable to the proton of the hydroperoxo ligand (Figure 4).[28,29]

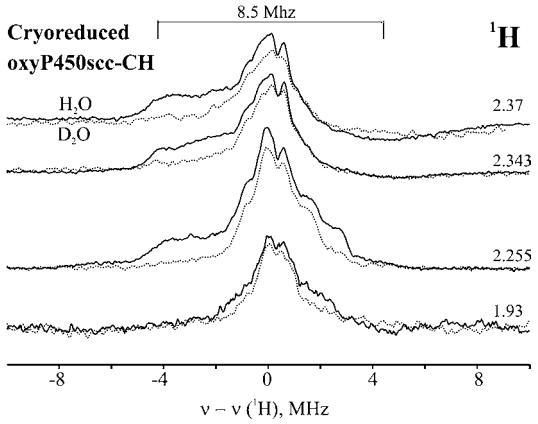

Figure 4. ^{1}H 35 GHz CW ENDOR spectra taken at indicated **g**-values of the cryoreduced oxy-P450scc-CH in 35% glycerol/H_2O buffer (pH 7.4) (solid line) and 35% glycerol-d_3/D_2O buffer (pH 7.0) (dotted line) annealed at 170 K for 2 min. Conditions: T = 2 K, 2 G, rf sweep rate = 1 MHz/s, bandwidth broadening = 60 kHz, 30 scans.

Two minor signals, **B** and **C**, are characterized by **g**-values of 2.214, 2.14 and 2.28, 2.156, respectively (Table 2). The **g**-values for **B** are typical of a peroxo-ferriheme intermediate,[8,28,31] while as shown below **C** is probably in the hydroperoxo-ferriheme state.[28,29] The observation of hydroperoxo-ferriheme state **A** as the main product of 77 K cryoreduction indicates that in the majority of the ternary oxy complex conformers that are the precursors to **A**, a hydrogen-bonding network tied to the precursor dioxygen ligand supports proton delivery, even at 77 K.[8,28−30,32] This was shown previously to imply the presence of an ordered water molecule in the vicinity of the distal oxygen of the O_2 ligand, as in the case of oxy-P450cam and oxy-heme oxygenase.[16,17,28,29] The majority hydroperoxo species **A** is stable during progressive annealing of the cryoreduced ternary CH complex at temperatures from 145 to 170 K. In contrast, during annealing at 145 K the peroxo-ferric intermediate **B** decays (Figure 3) in a fashion that can be described by a "stretched exponential", as is often the case,[33] and the decay slows by a factor of >5 in D_2O/glycerol-d_3 mixture (Figure 5). This

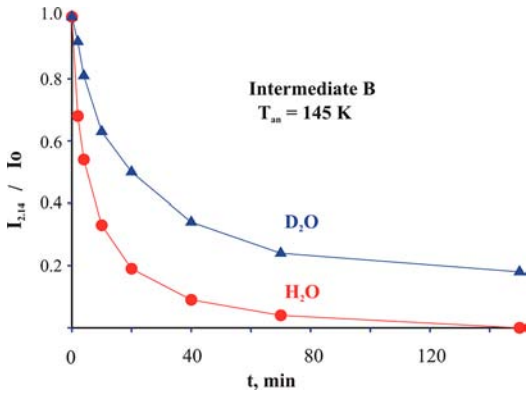

Figure 5. Kinetics of decay of the cryogenerated peroxo-ferriheme species **B** at 145 K in H_2O (red) and D_2O (blue) buffers at 145 K.

significant solvent kinetic isotope effect (sKIE) indicates that the rate-limiting step involves protonation of the peroxo ligand. Intermediate **C** also decays at 145 K but this process shows only a weak sKIE < 1.5 (Figure 6), suggesting proton-

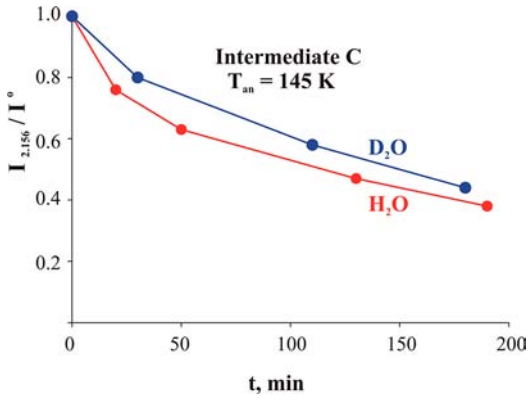

Figure 6. Kinetics of the decay of the intermediate **C** at 145 K in H_2O (red) and D_2O (blue) at 145 K.

independent structural changes in the active site of intermediate **C** during the relaxation. It appears that **B** and **C** both converted to a new species, **D**, during their decay. The **g**-values of **D** (Table 2, **g** = [2.37, 2.18, 1.94]) are characteristic of a hydroperoxy-ferriheme species, but with a slightly different environment than that of **A** (Figure 3, Table 2).

The hydroperoxo-ferric states **A** and **D** decay in parallel at 185 K (Figure 3). The data presented in Figure 7 show that this relaxation is characterized by sKIE ≥ 4. This behavior is expected if Cpd I is the active heme state. Heterolytic cleavage of the ferriheme hydroperoxy ligand to form the Cpd I, ferryl porphyrin π-cation radical, intermediate requires protonation of the distal hydroperoxy oxygen, and accordingly is expected to show a significant sKIE when protonation is the rate-limiting step, as observed here (Figure 7).

The loss of the hydroperoxo species is accompanied by the formation of a new species **G** which has two sub-states, the dominant one with **g** = [2.463, 2.257, 1.908]. The **g**-values of the two sub-states are the same as those of the EPR spectrum of the complex of ferric P450scc with 22-HC (Figure 3, Table 1).

dx.doi.org/10.1021/ja3067226 | J. Am. Chem. Soc. 2012, 134, 17149−17156

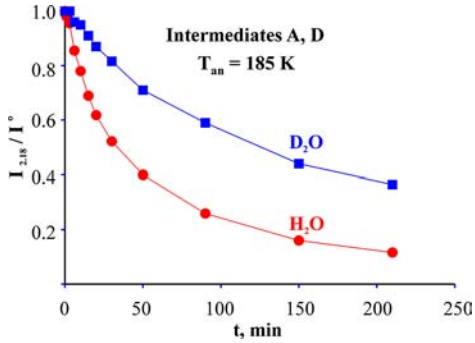

Figure 7. Kinetics of decays of hydroperoxy ferric intermediates **A** and **D** in H_2O (red) and D_2O (blue) at 185 K.

The only meaningful difference between the two spectra is in the relative proportions of the two sub-states: the primary product **G** forming after decay of the ferric hydroperoxo intermediates at 185 K contains relatively small amounts of the second conformer showing EPR signal with **g** = [2.44, 2.25, 1.92]. Thus we infer that CH has been hydroxylated during the annealing process and that species **G** is the product complex between ferric P450scc and 22-HC.

This assignment of intermediate **G** to the primary product complex is confirmed by the ^{1}H and ^{14}N ENDOR spectra for the **G** intermediate. As shown in Figure 8 the ^{1}H ENDOR

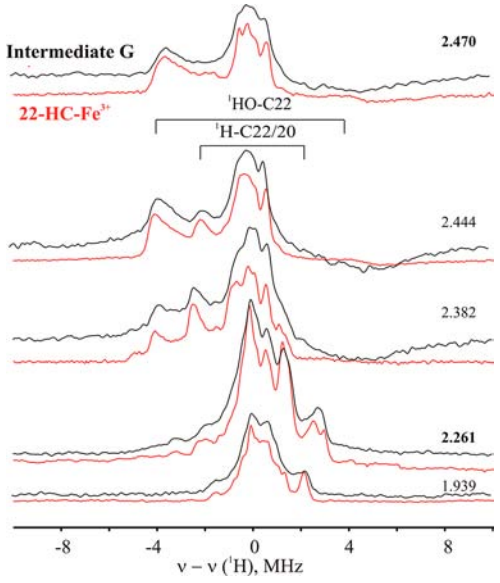

Figure 8. ^{1}H 35 GHz CW ENDOR spectra taken at indicated **g**-values for the intermediate **G** (black) and the complex of P450scc-22CH (red). Conditions: as in Figure 2.

spectrum of the dominant **G** sub-state is essentially the same as that obtained from the majority EPR signal of the 22-HC-ferric P450scc complex, with the same two resolved ^{1}H ENDOR signals, (A_{max} = 4.8 and ~8 MHz) (Figure S4). Likewise, the ^{14}N ENDOR spectra of the majority conformers of **G** and of the 22-HC-ferric P450scc complex are the same, and differ from that of the aquo-ferriheme complex in the presence of CH (Figure 2).

As illustrated in Figure 9, characterization of the coordination sphere of the ferriheme in the primary product, **G**, by ENDOR spectroscopy distinguishes between alternative active species,

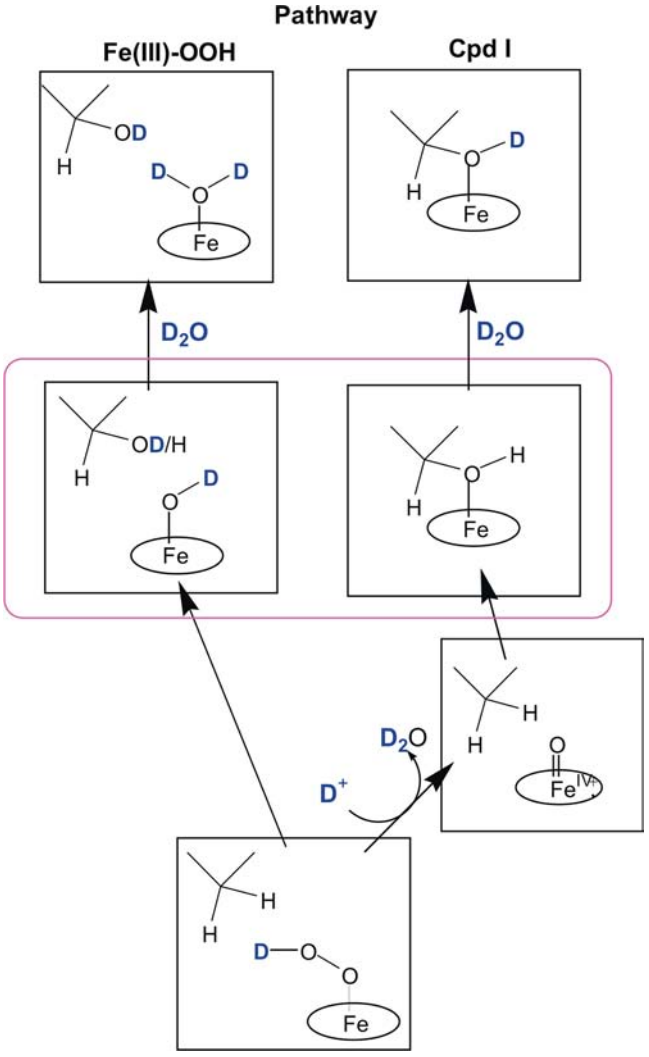

Figure 9. Schematic view of the reaction via the two alternative active oxygen species as carried out in D_2O buffer.

hydroperoxo-ferric or Cpd I. Insertion of an oxygen atom into CH by the ferryl ion of Cpd I should generate 22*R*-OH with its hydroxyl group bound to Fe(III). Moreover, the hydroxyl proton should be a ^{1}H that originates from a 22C-H of substrate, even if the reaction proceeds in D_2O buffer. In contrast, if the hydroperoxo-ferric heme intermediate is the hydroxylating species, the initial product state formed in D_2O buffer should contain D_xO bound to Fe, with the D derived from solvent.[8] In the ENDOR measurements on **G**, the ^{1}H signal with the larger coupling, which is associated with the heme-bound 22*R*-hydroxyl of 22-HC, is largely preserved when **G** is generated in D_2O buffer, Figure 10. This is as predicted when Cpd I is the hydroxylating agent (Figure 9) and previously found for P450cam.[28] These observations thus confirm that Cpd I is indeed the active species in hydroxylation of CH to form the 22-HC product.

During annealing at 220–240 K, intermediate **G** relaxes to the product complex in its equilibrium state, the only change being a decrease in the low-spin ferriheme sub-state with g_1 = 2.46–2.47 and an increase in the sub-state with g_1 = 2.44 and, yielding an EPR spectrum that is the same as that seen for the complex prepared by adding 22-HC to P450scc (Figure 3). Correspondingly, during relaxation of **G** to the equilibrium

dx.doi.org/10.1021/ja3067226 | J. Am. Chem. Soc. 2012, 134, 17149–17156

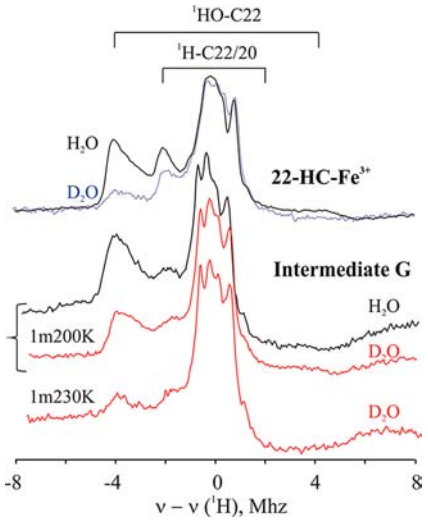

Figure 10. (A) ^{1}H 35 GHz CW ENDOR spectra of the complex of Fe(III) P450scc with 22-HC taken at g_1 = 2.44 in H_2O (solid) and D_2O (dotted). (B) ^{1}H 35 GHz CW ENDOR spectra of the primary product **G** taken at g_1 = 2.46 in H_2O (black) and D_2O (orange) trapped after annealing at 200 K for 1 min and at 230 K for 1 min. Conditions: as in Figure 2.

state at 230 K the 22*R*-hydroxyl proton signal disappears as exchange with D_2O solvent is enabled, but the signal assigned to the ^{1}H at either the C22 or C20 position of 22*R* remains (Figure 10). Taken together, the kinetic (Figure 7), EPR (Figure 3), and ENDOR (Figures 8, 10) observations strongly support the conclusion that Cpd I is the active hydroxylating species in P450scc catalytic conversion of CH into the 22-HC.

Interestingly, during annealing of the cryoreduced complex with CH no product complex is detected that has the **g**-values of the complex between P450scc and 20-HC. This observation is in agreement with the fact that the latter is only a minor product during metabolism of CH under physiological condition.[1,3]

DISCUSSION

This study provides new information about the structure of the oxy-heme center in the ternary oxy-P450scc-CH complex and about the mechanism of the first step in the conversion of CH to pregnenolone catalyzed by P450scc, the hydroxylation of CH to 22-HC.

Structure of the Oxy-heme Center. Cryoreduction of the oxy-P450scc-substrate complex at 77 K generates EPR-active states that retain the conformation of the oxy precursor[8,23,24,28−33] and thus provides a sensitive EPR/ENDOR probe of the diamagnetic oxy-ferrous precursor. The data presented here show that the ternary oxy-P450-CH complex exists in at least three different conformational sub-states that form spectroscopically distinct intermediates **A**, **B**, and **C** upon 77 K reduction (Figure 3, Table 2). EPR spectra show that the main products of radiolytic cryoreduction, species **A** and **C**, are distinct sub-states of the hydroperoxy-ferriheme state, with peroxo-ferriheme intermediate **B** a minor trapped product. As *in situ* cryoreduction of an oxy-heme must first form the peroxo-ferriheme species, the majority of cryoreduced oxy-heme conformers thus must undergo proton transfer at 77 K to form the observed **A** and **C** states.[8,34] Previous cryoreduction studies with a variety of oxy-hemoproteins, including cytochromes P450,[28,30,33] NOS,[23] heme oxygenase,[29,35] IDO/TDO[32] and oxy-globins[24,31,34,36] showed that such proton transfer to the basic peroxo ligand trapped at 77 K or below requires the presence in the parent oxy-hemoprotein of a hydrogen-bonded proton delivery network that includes an ordered water molecule in the active site that is hydrogen bonded to the terminal oxygen of the bound dioxygen ligand. This water serves as the proton shuttle to the peroxide ligand generated by cryoreduction at 77 K or below.[35,37−40] The transferred proton can originate from acid/base groups provided by amino acid residues within the active site,[28,29,35] from bound substrate,[23] or from water clusters connected to the active site by a proton delivery network.[41,42] Perturbation of this network in P450cam by site-specific mutation inhibits this proton delivery and inhibits conversion of cryogenerated peroxo to hydroperoxo species.[28] The nature of the substrate bound to P450cam was further shown to significantly modulate proton delivery and thereby lengthen the lifetime of the peroxo intermediate during annealing measurements.[33]

In case of gsNOS, bound NOHA stabilizes the enzymatically active, cryogenerated peroxo-ferriheme intermediate, whereas in the presence of Arg only the hydroperoxo species is formed at temperatures below 77 K.[23] Bound substrate was also shown to effectively inhibit protonation of the peroxo ligand in cryoreduced oxy-IDO and TDO.[24] Correspondingly, cryoreduction of oxy-globins, which do not have such a bound water, exclusively generates peroxo-ferric intermediates. In all cryogenerated peroxo intermediates of hemoproteins studied to date, the peroxo ligand forms an H-bond with a nearby amino acid residue (for instance, distal His in case of globins[31,36]) or bound substrate.[23,32] In the absence of such H-bonding interactions, a superoxy-ferrous species is trapped as the product of 77 K cryoreduction.[34] The peroxo ligand becomes protonated only at higher temperatures (for example, above 170 K in the oxy-globins),[36] at which a molecule of water might diffuse to the distal oxygen of the peroxo ligand.[32,36]

Overall, comparison with previous measurements on numerous proteins thus indicates that the ternary oxy-P450scc-CH complex contains an active-site water molecule that H-bonds to the terminal oxygen of the dioxygen ligand. This situation resembles that shown crystallographically for the oxy-P450cam-camphor complex, in which binding of dioxygen to the ferrous heme leads to incorporation of a water molecule that forms an H-bond to the distal oxygen of O_2,[16] and provides effective delivery of the first proton for monooxygenation at temperatures below 77 K.[28] The observation of the minor peroxo intermediate **B** along with the majority hydroperoxo products of cryoreduction indicates the additional presence of minority conformers of the ternary complex in which the H-bonding network to dioxygen is disrupted. However, the fact that protonation of the peroxo ligand nonetheless still occurs at the relatively low temperature of 120−145 K, where long-distance diffusion of a molecule water to the cryogenerated peroxo ligand is strongly hindered, suggests that these conformers likewise have a molecule of water incorporated in the vicinity of the dioxygen ligand, but that some minimal reorientation of this water is required to establish the required pathway for proton transfer.

Hydroxylation of Cholesterol. As with other monooxygenases[8] the cryoreduction approach to studying the hydroxylation of substrate by P450scc, is fully validated by (i) the demonstration that the cryoreduced ternary complex of oxy-P450scc-CH is catalytically competent and hydroxylates CH to form 22-HC and (ii) the absence of detectable

dx.doi.org/10.1021/ja3067226 | J. Am. Chem. Soc. 2012, 134, 17149−17156

formation of 20-HC, consistent with catalysis under physiological conditions. Controlled annealing of the cryogenerated hydroperoxo-ferriheme intermediates **A** and **C** enables a detailed examination of successive steps in CH hydroxylation by EPR and ENDOR spectroscopy. The initial intermediates formed by 77 K cryoreduction of the ternary oxy-P450scc-substrate complex, **A**, **B**, and **C**, relax to the two low-spin hydroperoxy-ferriheme species **A** and **D** (Table 2) upon annealing at 145−170 K. (Table 2) The existence of spectroscopic differences between species **A** and **D** indicates the presence of heterogeneity within the hydroperoxy-ferriheme site that likely reflects the corresponding heterogeneity of the oxy-heme structure. Further annealing at 185 K results in full conversion of both intermediates **A** and **D** into the primary product of hydroxylation, species **G**, which again exists in two sub-states. Both exhibit the same g tensors as the two sub-states of the equilibrium complex of ferric P450scc with 22-HC (Figure 3, Table 1) in which 22*R*-OH group is coordinated to the heme iron(III) at the distal axial position,[14,15] with **G** differing only in the relative proportions of the two sub-states (Figure 3).

Species **A** and **D** decay in parallel with a large solvent isotope effect, effective sKIE $\geq$ 4, which indicates that the rate-limiting step in this process is the proton-assisted reaction of hydroperoxo intermediate, as expected for conversion to Cpd I. The structure and isotopic composition of the primary product of hydroxylation trapped during progressive annealing, as determined by ENDOR spectroscopy, confirms that Cpd I is indeed the catalytically active heme species.

Previous studies of P450cam and gsNOS[8,23,28,33] showed that the newly formed hydroxyl group of the hydroxylated product is coordinated to the ferric heme iron in the nonequilibrium primary product state when the ferryl moiety of Cpd I is the active species. In contrast, hydroxylation of substrate by the peroxo/hydroperoxo moiety involves an concerted insertion of the distal peroxy/hydroperoxy oxygen into substrate and would generate a primary product state with a hexa-coordinate ferric heme moiety with water/hydroxide as the sixth axial ligand.[8] This scenario describes heme hydroxylation by cryoreduced oxy-HO.[29]

With this foundation, the ^{1}H ENDOR data collected from the primary product of hydroxylation, **G**, formed during annealing at 200 K in deuterated solvent (Figure 10), establish that Cpd I is the hydroxylating agent. The insertion of oxygen into CH the C22−H bond by the ferryl moiety of enzyme in deuterated solvent must yield 22-HC, C22-OH as product, rather than 22-HC, C22-OD, which would be the product if deuterated hydroperoxy intermediate (FeOOD) were the active species (Figure 9). In fact, the primary product **G** formed with the enzyme in a D_2O/glycerol-d_3 mixture shows a strong ^{1}H ENDOR signal from the coordinated hydroxyl of 22-HC, and that this exchanges for D during annealing at higher temperatures. This is precisely as expected (Figure 9) if the ferryl oxygen inserted in the C−H bond of substrate (Figure 10). Failure to detect Cpd I by EPR during this process can be accounted for by a high rate of reaction with bound substrate, which prevents its accumulation.

In the final stage of annealing **G**, the nonequilibrium proportions of the two conformations of 22-HC coordinated to heme iron(III) relax to the equilibrium proportions upon annealing at 240 K (Figure 3).

In this picture, the hydroperoxo-ferriheme intermediate undergoes the key O−O bond-breaking reaction. Comparison of the spin-Hamiltonian parameters for the hydroperoxo-ferriheme as generated in different proteins/enzymes thus affords an opportunity to consider the properties of this state. As discussed earlier, the peroxo- and hydroperoxo-ferrihemes exhibit low-spin ferriheme EPR spectra that are distinguished by g_1: $g_1 < 2.27$ for peroxo and $g_1 \geq 2.28$ for hydroperoxo. As shown in Table S1, the range of values observed to date for hydroperoxo-ferrihemes, $2.28 \leq g_1 \leq 2.37$ is essentially the same for proteins with proximal histidyl and cysteinyl ligands, suggesting that the proximal ligand plays essentially no role in determining the *ground-state* electronic structure of this species, unlike the case of the aquaferriheme form.

The values of g_1 for heme oxygenase, for which the active oxygen species is the hydroperoxo-ferriheme, and for P450scc-CH, for which Cpd I is the active oxygen species, are essentially the same, suggesting that the *ground-state* electronic structure of the Fe-OOH moiety plays little role in determining the fate of this state, and hence the ultimate active oxygen species. This supports the suggestion that the fate of the Fe-OOH is determined by a kinetic competition between heterolytic bond cleavage to form Cpd I, versus direct reaction with substrate (substrate modulation of reactivity),[33] as influenced by the properties of the heme pocket.[8]

SUMMARY

Cryoreduction/annealing experiments in combination with EPR/ENDOR spectroscopy have demonstrated that Compound I is the reactive species during P450scc-catalyzed hydroxylation of cholesterol to 22*R*-hydroxycholesterol. The cryoreduction experiments further indicate the presence of the proton delivery network which includes an ordered water molecule that is H-bonded to the distal oxygen of the dioxygen ligand in the ternary oxy-P450scc-CH complex, and which provides efficient proton transfer to the one electron reduced oxy-heme site.

ASSOCIATED CONTENT

Supporting Information

One scheme and six EPR and ENDOR figures. This material is available free of charge via the Internet at http://pubs.acs.org.

AUTHOR INFORMATION

Corresponding Author

usanov@iboch.bas-net.by; bmh@northwestern.edu

Notes

The authors declare no competing financial interest.

ACKNOWLEDGMENTS

We thank the NIH for support (HL13531, B.M.H.) and Prof. H. Halpern, Pritzker School of Medicine, University of Chicago, for access to the ^{60}Co Gamma cell irradiator.

REFERENCES

(1) Bernhardt, R.; Waterman, M. R. In *Metal Ions in Life Science*; Sigel, A., Sigel, H., Sigel, R. K., Eds.; John Wiley and Sons: New York, 2007; Vol. 3, p 361.

(2) Gilep, A. A.; Sushko, T. A.; Usanov, S. A. *Biochim. Biophys. Acta: Proteins Proteom.* **2011**, *1814*, 200.

(3) Tuckey, R. C. *Placenta* **2005**, *26*, 273.

(4) De Montellano, P. R. O.; De Voss, J. J. *Nat. Prod. Rep.* **2002**, *19*, 477.

(5) Denisov, I. G.; Makris, T. M.; Sligar, S. G.; Schlichting, I. *Chem. Rev.* **2005**, *105*, 2253.

(6) Hlavica, P. *Eur. J. Biochem.* **2004**, *271*, 4335.
(7) Akhtar, M.; Njar, V. C. O.; Wright, J. N. *J. Steroid Biochem. Mol. Biol.* **1993**, *44*, 375.
(8) Davydov, R.; Hoffman, B. M. *Arch. Biochem. Biophys.* **2011**, *507*, 36.
(9) Jung, C. *Biochim. Biophys. Acta* **2011**, *1814*, 46.
(10) Gantt, S. L.; Denisov, I. G.; Grinkova, Y. V.; Sligar, S. G. *Biochem. Biophys. Res. Commun.* **2009**, *387*, 169.
(11) Kellner, D. G.; Hung, S.-C.; Weiss, K. E.; Sligar, S. G. *J. Biol. Chem.* **2002**, *277*, 9641.
(12) Spolitak, T.; Funhoff, E. G.; Ballou, D. P. *Arch. Biochem. Biophys.* **2010**, *493*, 184.
(13) Rittle, J.; Green, M. T. *Science* **2010**, *330*, 933.
(14) Strushkevich, N.; MacKenzie, F.; Cherkesova, T.; Grabovec, I.; Usanov, S.; Park, H.-W. *Proc. Natl. Acad. Sci. U.S.A.* **2011**, *108*, 10139.
(15) Mast, N.; Annalora, A. J.; Lodowski, D. T.; Palczewski, K.; Stout, C. D.; Pikuleva, I. A. *J. Biol. Chem.* **2011**, *286*, 5607.
(16) Schlichting, I.; Berendzen, J.; Chu, K.; Stock, A. M.; Maves, S. A.; Benson, D. E.; Sweet, B. M.; Ringe, D.; Petsko, G. A.; Sligar, S. G. *Science* **2000**, *287*, 1615.
(17) Matsui, T.; Unno, M.; Ikeda-Saito, M. *Acc. Chem. Res.* **2010**, *43*, 240.
(18) Kuehnel, K.; Derat, E.; Terner, J.; Shaik, S.; Schlichting, I. *Proc. Natl. Acad. Sci. U.S.A.* **2007**, *104*, 99.
(19) Lepesheva, G. I.; Usanov, S. A. *Biochemistry (Moscow)* **1998**, *63*, 224.
(20) Lepesheva, G. I.; Strushkevich, N. V.; Usanov, S. A. *Biochim. Biophys. Acta: Protein Struct. Mol. Enzymol.* **1999**, *1434*, 31.
(21) Glasoe, P. K.; Long, F. A. *J. Phys. Chem.* **1960**, *64*, 188.
(22) Tuckey, R. C.; Kamin, H. *J. Biol. Chem.* **1982**, *257*, 9309.
(23) Davydov, R.; Sudhamsu, J.; Lees, N. S.; Crane, B. R.; Hoffman, B. M. *J. Am. Chem. Soc.* **2009**, *131*, 14493.
(24) Davydov, R.; Osborne, R.; Shanmugam, M.; Du, J.; Dawson, J.; Hoffman, B. *J. Am. Chem. Soc.* **2010**, *132*, 14995.
(25) Orme-Johnson, N. R.; Light, D. R.; White-Stevens, R. W.; Orme-Johnson, W. H. *J. Biol. Chem.* **1979**, *254*, 2103.
(26) Takeuchi, K.; Tsubaki, M.; Futagawa, J.; Masuya, F.; Hori, H. *J. Biochem.* **2001**, *130*, 789.
(27) Lipscomb, J. D. *Biochemistry* **1980**, *19*, 3590.
(28) Davydov, R.; Makris, T. M.; Kofman, V.; Werst, D. W.; Sligar, S. G.; Hoffman, B. M. *J. Am. Chem. Soc.* **2001**, *123*, 1403.
(29) Davydov, R.; Kofman, V.; Fujii, H.; Yoshida, T.; Ikeda-Saito, M.; Hoffman, B. *J. Am. Chem. Soc.* **2002**, *124*, 1798.
(30) Davydov, R.; Razeghifard, R.; Im, S.-C.; Waskell, L.; Hoffman, B. M. *Biochemistry* **2008**, *47*, 9661.
(31) Davydov, R.; Kofman, V.; Nocek, J.; Noble, R. W.; Hui, H.; Hoffman, B. M. *Biochemistry* **2004**, *43*, 6330.
(32) Davydov, R. M.; Chauhan, N.; Thackray, S. J.; Anderson, J. L. R.; Papadopoulou, N. D.; Mowat, C. G.; Chapman, S. K.; Raven, E. L.; Hoffman, B. M. *J. Am. Chem. Soc.* **2010**, *132*, 5494.
(33) Davydov, R.; Perera, R.; Jin, S.; Yang, T.-C.; Bryson, T. A.; Sono, M.; Dawson, J. H.; Hoffman, B. M. *J. Am. Chem. Soc.* **2005**, *127*, 1403.
(34) Davydov, R.; Satterlee, J. D.; Fujii, H.; Sauer-Masarwa, A.; Busch, D. H.; Hoffman, B. M. *J. Am. Chem. Soc.* **2003**, *125*, 16340.
(35) Davydov, R.; Chemerisov, S.; Werst, D. E.; Rajh, T.; Matsui, T.; Ikeda-Saito, M.; Hoffman, B. M. *J. Am. Chem. Soc.* **2004**, *126*, 15960.
(36) Kappl, R.; Höhn-Berlage, M.; Hüttermann, J.; Bartlett, N.; Symons, M. C. R. *Biochim. Biophys. Acta* **1985**, *827*, 327.
(37) Kumar, D.; Hirao, H.; De, V. S. P.; Zheng, J.; Wang, D.; Thiel, W.; Shaik, S. *J. Phys. Chem. B* **2005**, *109*, 19946.
(38) Vidossich, P.; Fiorin, G.; Alfonso-Prieto, M.; Derat, E.; Shaik, S.; Rovira, C. *J. Phys. Chem. B* **2010**, *114*, 5161.
(39) Li, H.; Igarashi, J.; Jamal, J.; Yang, W.; Poulos, T. L. *JBIC, J. Biol. Inorg. Chem.* **2006**, *11*, 753.
(40) Cho, K.-B.; Derat, E.; Shaik, S. *J. Am. Chem. Soc.* **2007**, *129*, 3182.
(41) Guallar, V.; Harris, D. L.; Batista, V. S.; Miller, W. H. *J. Am. Chem. Soc.* **2002**, *124*, 1430.
(42) Bonin, J.; Costentin, C.; Louault, C.; Robert, M.; Saveant, J.-M. *J. Am. Chem. Soc.* **2011**, *133*, 6668.